ADVANCED MATERIALS
www.advmat.de

All-Organic and Fully-Printed Semitransparent Photodetectors Based on Narrow Bandgap Conjugated Molecules

Giuseppina Pace, Andrea Grimoldi, Dario Natali, Marco Sampietro, Jessica E. Coughlin, Guillermo C. Bazan, and Mario Caironi**

The multiple potentials offered by organic electronics have been well described in terms of chemically tailored properties, mechanical flexibility, earth abundance of the basic materials, solution processability and low cost. Formulated into functional inks, organic semiconductors can be processed with printing technologies, thus allowing scalable device fabrication across large-area and onto flexible substrates, opening a complete new pathway for organic electronics and its integration into circuits.[1,2] Organic electronics therefore enables a manifold of novel and alternative applications in portable, mechanically robust, and light-weight devices. In particular, in the case of organic photodetectors, all-plastic short range data communication, plastic digital and conformable imagers, position and security sensors, and interactive surfaces become possible.[1] To date the examples of all-printed photoresponsive devices are scarce,[2,3] and limited to the case of blends comprising conjugated polymer donors. Semiconducting small molecules are also appealing, as they are not affected by polydispersity and are characterized by a simpler purification technique, which also fulfill the purpose of a better scalability of organic electronics. While inkjet printed blends of semiconducting polymers have already been shown to be reproducible,[4,5] additional issues have to be solved when dealing with the printing of small molecule-based blends. The major problem arises from the strong tendency of such small molecules to crystallize. Crystalline films are desired when the printing is directed to specific functionalities of the organic films, as in high mobility, single crystal organic field effect transistors (OFET).[6,7] Instead in donor acceptor blends a proper phase intermixing is required to improve charge separation.[8] However, the strong tendency of small molecules to crystallize usually limits the control of the uniformity and the reproducibility of the printed film. In fact, a marked tendency to crystallization may lead to strong phase segregation between donor and acceptor components (D-A) in the blend. Such poor intermixing reduces the D-A interfacial area, thus limiting exciton dissociation and therefore charge collection at the electrodes. Also, the presence of large aggregates or crystallites very often increases the roughness of the active materials favoring short circuiting and higher densities of interfacial defects. Furthermore, solutions containing small molecules are characterized by a lower viscosity than polymer solutions, providing a very different rheological behavior of the printed drop, favoring coffee stain flows.[9,10]

In this work we make use of a recently synthesized narrow band-gap small molecule and we achieve reproducible printing by introducing a semiconducting polymer to obtain a ternary blend. Concerning photoactive blends based on small molecules, this is a quite novel strategy and allowed us to greatly reduce issues related to poor printability and low device performances. We demonstrate an all-organic and fully-printed photodiode, with a spectral responsivity region extending until 750 nm, which thanks to semitransparent contacts enables double-side signal detection: light detection is indeed demonstrated to occur both when light is incoming from the top and from the bottom side of the photodiode, with comparable efficiencies.

Narrow band-gap small molecules have been successfully employed in organic solar cells as they can combine IR photoresponse, high power conversion efficiencies and ease of processability due to their higher solubility with respect to polymers.[11] Recently, a blend of 7,7′-(4,4-bis(2-ethylhexyl)-4H-silolo[3,2-b:4,5-b′]dithiophene-2,6-diyl)bis(6-fluoro-4-(5′-hexyl-[2,2′-bithiophen]-5-yl) benzo[*c*][1,2,5] thiadiazole) (T1) and [6,6]-phenyl-C_{70}-butyric acid methyl ester ($PC_{70}BM$) in the presence of the additive 1,8-diiodiooctane has been demonstrated to provide solar cells with power conversion efficiencies of up to 9 %.[12–14]

Firstly, we investigated the inkjet printing of binary blends based on T1 acting as donor and $PC_{70}BM$ as the acceptor dissolved in dichlorobenzene-mesitylene solvent mixture. This solvent combination results in a strong coffee stain effect, leaving the central part of the printed stripe thinner than 30 nm, and edges as thick as 80 nm. The binary formulation has also been

G. Pace,[+] A. Grimoldi,[+] D. Natali, M. Sampietro, M. Caironi
Center for Nano Science and Technology@PoliMi
Istituto Italiano di Tecnologia
Via Pascoli 70/3
20133, Milano, Italy
E-mail: giuseppina.pace@iit.it; mario.caironi@iit.it
A. Grimoldi, D. Natali, M. Sampietro
Dipartimento di Elettronica
Informazione e Bioingegneria
Politecnico di Milano, P.za L. Da Vinci
32 20133, Milano, Italy
J. E. Coughlin, G. C. Bazan
Center for Polymers & Organic Solids
University of California
Santa Barbara, CA, 93106-5090, USA
[+]These authors contributed equally to this work

DOI: 10.1002/adma.201402918

tested with other solvents as chlorobenzene, but always resulted in a high probability of nozzle clogging due to the likelihood of precipitate formation. The coffee ring effect was difficult to overcome by using a suitable mixing of solvents with different boiling points and surface tensions, which is a strategy commonly adopted in the case of polymer semiconductor blends.[2] The profile of the drop obtained by inkjet printing the binary blend T1:$PC_{70}BM$ dissolved in a mesitylene-dichlorobenzene solvent mixture is reported in the Supporting Information (Figure S2). When integrated into a vertical structured device, where the printed layer is sandwiched between two conducting electrodes, such active layers lead to very unstable electrical behavior, prone to short-circuiting even at low bias voltages, likely due to a too thin and defective active layer (see SI for details). The thickness of the layer can be increased by heating the substrate up to 120 °C during printing. Such a thick film could form thanks to the increased vapor pressure of the solvents at high temperature, favoring the fast drying of the printed drop coming into contact with the hot substrate plate and limiting the spreading of the ink. However, this causes strong phase separation together with the formation of large T1 crystals (**Figure 1**a), providing very low device reproducibility.[15] To overcome this issue we adopted a ternary formulation, where an additional photoactive polymer is introduced into the blend to vary the ink viscosity and to reduce small molecule crystallization. To this end we chose P3HT (Poly(3-hexylthiophene-2,5-diyl)) as the semiconducting polymer, due to its capability to participate to the transport of the photogenerated charges. Also, it is widely commercially available and cost-effective photoactive material, providing the possibility to foster a broadband response of the device when combined with T1. The new ternary blend formulation allowed a reduction in the coffee ring effect by favoring a better control on the printing process. This allowed us to reproducibly print blend stripes with uniform thicknesses of about 100 nm by holding the substrate at room temperature. Following recent studies presented in the literature,[16,17] we have also explored the possibility to introduce a high molecular weight and insulating polystyrene (PS) polymer to increase the solution viscosity. Huang *et al.*[16] showed that for low PS concentrations it is possible to improve the thickness, the absorbance and the uniformity of films based on T1:$PC_{71}BM$ deposited by spin-coating. However, by employing a similar strategy we could not easily optimize inkjet printable formulations due to high viscosity. A deeper investigation of the role played by molecular weight and concentration of PS was not the purpose of this work.

Different amounts of P3HT were added to the ternary blend: for a 1 mL solution we kept the amounts of T1 (15 mg mL^{-1}) and $PC_{70}BM$ (14 mg mL^{-1}) constant, to which 2, 5 and 10 mg of P3HT was added (respectively 10%, 26%, 53% weight ratio of P3HT and binary blend). The AFM image of the T1:$PC_{70}CM$ photoactive film (Figure 1a) shows features similar to the ones exhibited by crystalline films of the same materials, as previously obtained by other groups,[15,18,19] leading to the conclusion that also in the printed film of this work the T1 component has a strong tendency to crystallize. By increasing the amount of P3HT an effective morphology variation occurs and the crystallinity of T1 is strongly affected. Crystalline domains are still evident for blends containing 10% P3HT. Their size reduces by adding 26 % of P3HT, while they are no more identifiable for 53% P3HT addition. This last ink formulation led to a printed layer morphology with evident fibrillar structures, ascribable to P3HT aggregates.[20] This trend is also confirmed by UV-Vis absorption spectra reported in **Figure 2**, where the main absorption of the T1 around 400 nm shifts to lower wavelength upon increasing the P3HT content, as expected for a less crystalline film of T1.[15,19] Though the visible region of the spectra of T1 in the blends overlaps with the P3HT absorption tail, the relative intensity of the peaks around 600 nm and 700 nm suggests the same reduced crystallization of T1 when increasing the P3HT content in the blend. This variation in the relative intensity of the peaks at 600 nm and 700 nm and the shift in the blue region were already shown for samples of pristine T1 owing to different degree of crystallinity.[19]

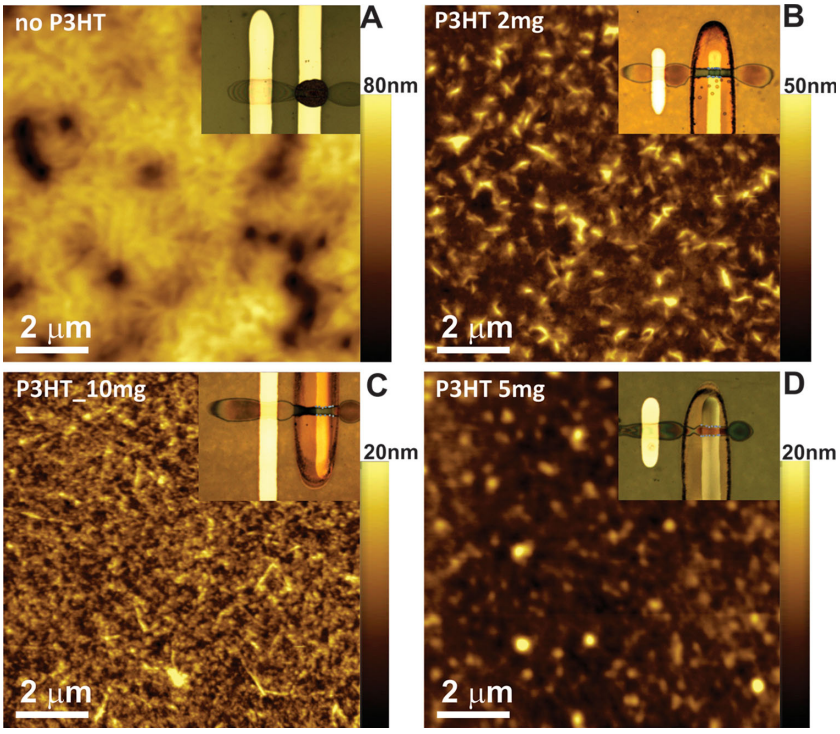

Figure 1. AFM images of inkjet printed blends on top of the silver electrode: a) T1:$PC_{70}BM$ in the absence of P3HT. The substrate was heated up to 120 °C during printing; b) T1:$PC_{70}BM$ blend with the addition of 2 mg of P3HT; c) T1:$PC_{70}BM$ blend with the addition of 5 mg of P3HT; d) T1:$PC_{70}BM$ blend with the addition of 10 mg of P3HT. Inset: optical microscope images of the printed photodetectors; the brighter vertical stripes are Ag printed bottom electrodes; the horizontal semitransparent stripes are the PEDOT:PSS top electrodes; the blend stripe is printed on top of the Ag electrode (longitudinal line in figures B-C-D, in figure A the blend is the dark drop).

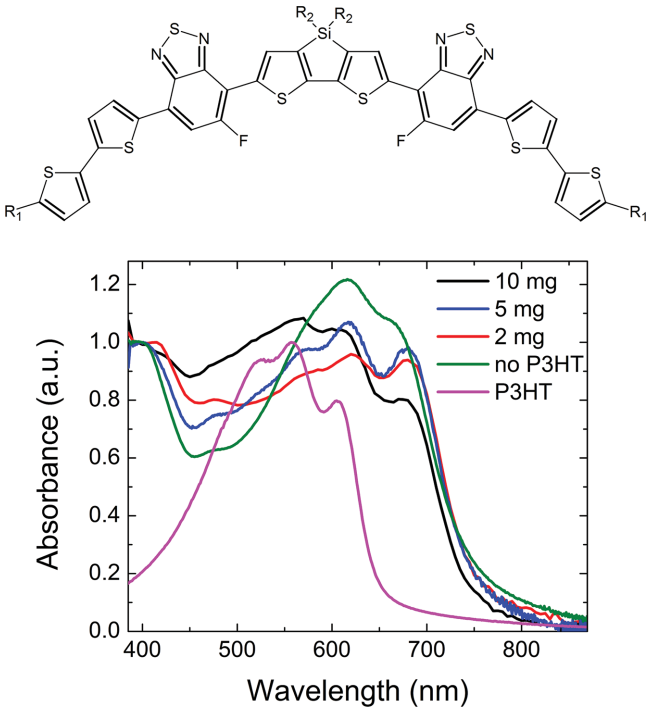

Figure 2. Top: chemical structures of T1 (R_1 = n-hexyl R_2 = 2-ethylhexyl). Bottom: UV-Vis absorption spectra of the printed blend on a PEN substrate covered with a layer of PFN, normalized at 400 nm. The PEN-PFN absorption has been subtracted as background.

Once we optimized the ink formulation, we fabricated the photodetector devices on flexible and transparent polyethylene naphthalate (PEN) substrates. The devices have a vertical structure with the photoactive layer placed between two conductive electrodes. Electrodes were realized by printing commercial inks: a silver nanoparticle based ink for the bottom opaque electrodes or poly(3,4-ethylene dioxythiophene):(polystyrene sulfonic acid) (PEDOT:PSS) for the transparent ones. In all the devices the top contact is a printed PEDOT:PSS electrode (sheet resistance ~ 5.5 kΩ/square). Current versus voltage measurements (*IV*) for devices based on printed ternary blends are provided in **Figure 3**a, along with the corresponding External Quantum Efficiency (EQE) spectra in Figure 3b. For photodetectors, the printed bottom electrode was functionalized with poly[(9,9-bis(3′-(N,N-dimethylamino)propyl)-2,7-fluorene)-alt-2,7-(9,9–dioctylfluorene)] (PFN) by means of spincoating. As reported in the literature for other polyelectrolytes,[21] PFN plays a significant role in charge injection and extraction at the interface between electrodes and organic semiconductors.[22] The introduction of PFN in our devices led to a rectifying behavior by strongly decreasing the inverse dark current and thus increasing the ON/OFF ratio. In the Supporting Information we provide a more comprehensive description of the role played by the PFN interlayer. In particular, we could identify an effective hole-injection blocking effect. We investigated hole only devices where hole injection was favored due to the choice of a Au bottom electrode. Such devices demonstrate that when PFN is facing the hole injecting electrode, the dark current density is strongly reduced with respect to the device with no PFN interlayer. This conclusion is supported by Kelvin probe

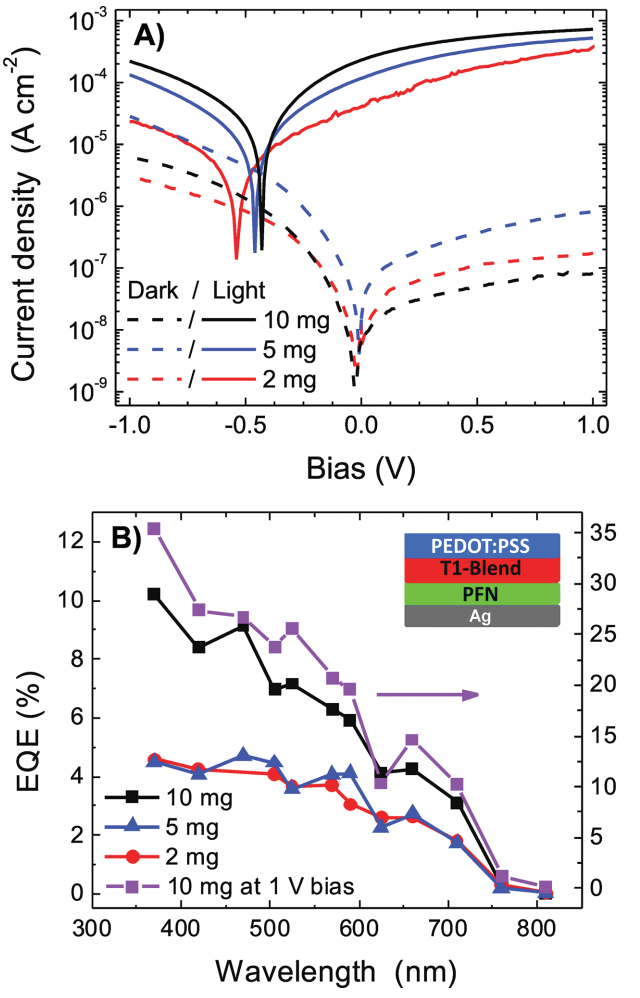

Figure 3. A) dark and white light (5 mW cm^{-2}) *IV* of the devices with printed Ag bottom electrode; B) EQE spectra at 0 V and 1 V. (The 1 V EQE for 5 mg and 2 mg of P3HT are reported in the SI). Inset: scheme of photodetector layered structure.

measurements where we measured a decreased work-function for both Au and PEDOT:PSS electrodes, following the PFN layer deposition. This further confirms the effective reduction of hole injection from PFN functionalized electrodes. Photodiodes made with the 53% P3HT ink formulation showed the best performances in terms of dark current and photocurrent density approaching light-dark current ratio of 10^4, while the V_{OC} is only slightly reduced (Figure 3a). Measurements of EQE spectra were performed at 0 V and 1 V (Figure 3b and SI). Higher photoresponse in the 650–750 nm region occurs when increasing the P3HT content in the blend. In this region only the T1 is responsible for the light absorption. By combining these data with the observation of a decreased crystallinity of T1, we find, as expected, that the strong tendency of small molecules to crystallize can be a drawback when trying to optimize the photodetector efficiency.

So far we have demonstrated that it is possible to obtain high efficiency in small molecule printed photodetectors through the addition of a semiconducting polymer that inhibits crystallization. To fully exploit the potential of our approach and

the added value of organic printing technology, we have optimized an all-carbon based photodetector printed on flexible substrates with semitransparent electrodes.[23] For this goal we replaced the silver bottom contact with a PEDOT:PSS electrode, so that the only non transparent material would be the active blend for which the transparency could be modulated by varying the thickness. Not only does this electrode allow for the semi-transparency of the device, but it also provides a very smooth interface with the organic semiconductor. This feature reduces instabilities due to the formation of leakage paths often observed with the rougher silver printed electrode. The rectifying behavior and the dark current density, as low as 1 μA cm^{-2} (**Figure 4**a), shown by these devices, prove that the PFN interlayer is effective in inducing asymmetry between top and bottom electrode work functions as also demonstrated by Kelvin probe measurements (SI). Figure 4b reports the EQE measurements acquired with light impinging respectively from the top side and bottom side of the device. We stress that the semi-transparent photodetector responds from both sides to a broad wavelength band up to 750 nm with an EQE above 10%. To demonstrate the generality of this approach towards double-side detectors, we also fabricated semitransparent fully organic photodetectors based on P3HT:$PC_{61}BM$ blend with 100 nA cm^{-2} dark current density and a maximum EQE of 60% (see Supporting Information for more details).

In conclusion, this work demonstrates the possibility to reproducibly fabricate all-organic and fully-printed, semi-transparent photodiodes on plastic substrates by adopting low band gap small molecule based inks, properly formulated by exploiting ternary blends containing semiconducting polymers. A broad-band wavelength response could be obtained when light impinges both from the top and from the bottom side. Semi-transparent, all-printed detectors can pave the way for a cost-effective integration of innovative light sensing elements in future interactive surfaces, flexible displays, and surveillance systems.

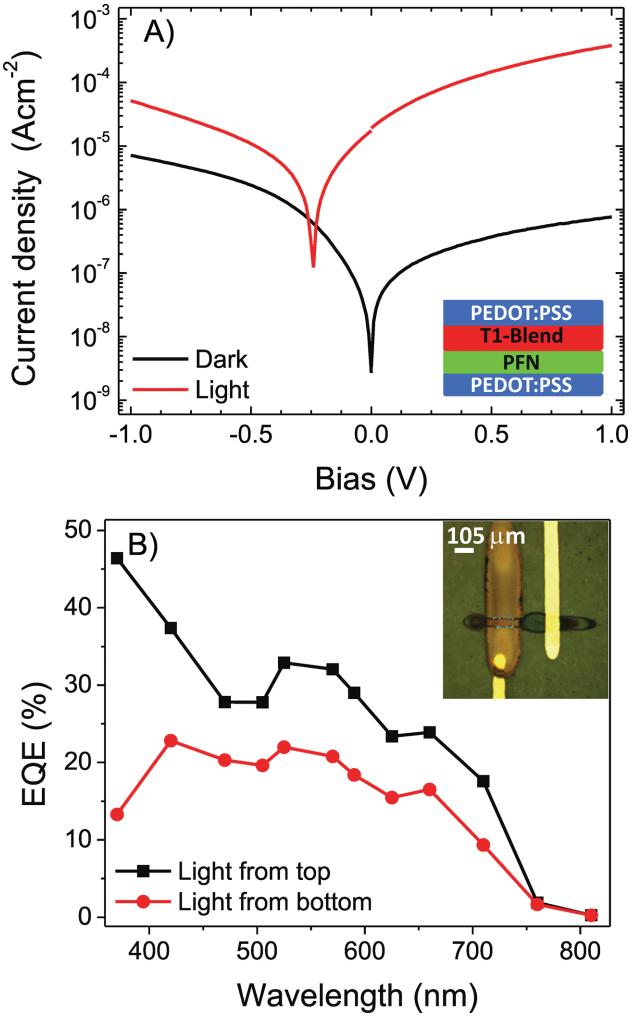

Figure 4. A) Dark and Light *IV* of the devices with bottom and top PEDOT:PSS electrodes for blend containing 5 mg of P3HT. Inset: scheme of the semi-transparent phodetector layered structure. B) EQE spectra of the device acquired at 1 V bias, with light impinging either from the bottom or the top side. Inset: optical microscope image of all-organic photodetector. The different values found in the EQE for top and bottom side illumination is still under investigation. This could be associated with a possible vertical phase segregation of the $PC_{70}BM$ to the bottom electrodes acting as a screening for the incoming light reducing the effective photon intensity absorbed by the blend. Also, when shining light from the bottom electrode, the PEN substrate can act as a scattering medium reducing the effective light intensity impinging on the active layer.

Experimental Section

Polyethylene naphthalate (PEN) was purchased from DuPont and used as flexible, lightweight and transparent substrate. The synthesis of T1 has already been reported.[13] The silver layer was inkjet printed using a Fujifilm Dimatix 10 pl cartridge filled with Cabot Conductive Ink CCI-300 further diluted with ethanol and ethylene glycol (1:0.3:0.7), filtered with 0.2 μm PTFE filter. After deposition, two annealing steps were performed in ambient atmosphere, the first one at 70 °C for 30 minutes, the second one at 140 °C for 10 minutes. PFN was purchased from Ossila and dissolved in a mixture of methanol (99.6% vol.) and acetic acid (0.4 % vol.) to obtain a 1 mg mL^{-1} solution which was deposited by spincoating at 2500 rpm for 1 min with an acceleration of 1000 rpm s^{-1}. The measured thickness of the PFN layer on glass was 5 nm. The concentration of the binary blend of T1 and $PC_{70}BM$ was 35 mg mL^{-1} (21 mg mL^{-1} of T1 and 14 mg mL^{-1} of $PC_{70}BM$). The ternary blend of T1, $PC_{70}BM$ (purity 99% from Solenne) and P3HT were prepared from a solution of 1,2-dichlorobenzene (68% vol.) and mesitylene (32% vol.) to which a 0.4 vol % of diiodoctane (Sigma Aldrich) was added. All solvents where purchased from Sigma Aldrich. P3HT (RR = 96.6%, MW = 65500 Dalton) was purchased from Merck. The blend solution was stirred overnight at 100 °C in glovebox. Before printing, the solution was heated at 70 °C for 10 min, filtered with a 0.2 μm PTFE filter and then printed with a Microfab JETLAB 4 equipped with a 40 μm diameter nozzle with Diamond Like Carbon (DLC) coating. Clear solutions were obtained upon addition of P3HT, no particulate suspension was present. The new formulation remained clear and stable throughout all the printing time. Clevios P Jet N PEDOT:PSS ink was enriched with Zonyl FS-300 fluorosurfactant, filtered with 0.2 μm PVDF filter and used to load a Dimatix 10 pl cartridge. The PEDOT:PSS bottom electrode was annealed at 100 °C for 10 min before blend printing. Each deposition was performed in ambient condition. KLA Tencor Alpha-Step IQ was used to measure stripes profile. The UV-Vis absorption spectra were acquired on a Varian Cary 50 Spectrophotometer. *IV* measurements in dark and under white light (6400 K, 5 $mWcm^{-2}$) were performed in glovebox and acquired with an Agilent B1500A Semiconductor Parameter Analyzer. EQE measurements were performed in glovebox at

incident power of about 5 mW cm^{-2}. Devices were illuminated by a set of Light Emitting Diodes covering the spectral range between 370 nm and 810 nm. Atomic Force Microscopy (AFM) images were acquired with an Agilent 5500 microscope.

Supporting Information

Supporting Information is available from the Wiley Online Library or from the author.

Acknowledgements

The authors are thankful to J. Ball for his help in the revision of the manuscript. Fondazione Cariplo is acknowledged for financial support through the InDiXi project grant n. 2011-0368. M. C. acknowledges financial support from European Union through the Marie-Curie Career Integration Grant 2011 "IPPIA", within the EU Seventh Framework Programme (FP7/2007-2013) under grant agreement No. PCIG09-GA-2011-291844. Work at UCSB was supported by the Institute for Collaborative Biotechnologies through grant W911NF-09-0001 from the U.S. Army Research Office. The content of the information does not necessarily reflect the position or the policy of the Government, and no official endorsement should be inferred.

Received: July 1, 2014
Revised: July 28, 2014
Published online: September 2, 2014

[1] K. J. Baeg, M. Binda, D. Natali, M. Caironi, Y. Y. Noh, *Adv. Mater.* **2013**, *25*, 4267.
[2] G. Azzellino, A. Grimoldi, M. Binda, M Caironi., D. Natali, M. Sampietro, *Adv. Mater.* **2013**, *25*, 6829.
[3] A. C. Arias, J. D. MacKenzie, I. McCulloch, J. Rivnay, A. Salleo, *Chem. Rev.* **2010**, *110*, 3.
[4] A. Teichler, J. Perelaer, U. S. Schubert, *J. Mater. Chem. C* **2013**, *1*, 1910.
[5] A. Teichler, J. Perelaer, F. Kretschmer, M. D. Hager, U. S. Schubert, *Macromol. Chem. Phys.* **2013**, *214*, 664.
[6] K. Fukuda, Y. Takeda, M. Mizukami, D. Kumaki, S. Tokito, *Sci Rep-Uk* **2014**, 4.
[7] Y. H. Kim, B. Yoo, J. E. Anthony, S. K. Park, *Adv. Mater.* **2012**, *24*, 497.
[8] H. Hoppe, N. S. Sariciftci, *J. Mater. Chem.* **2006**, *16*, 45.
[9] R. D. Deegan, O. Bakajin, T. F. Dupont†, G. Huber, S. R. Nagel, T. A. Witten, *Nature* **1997**, *289*, 327.
[10] L. Y. Cui, J. H. Zhang, X. M. Zhang, L. Huang, Z. H. Wang, Y. F. Li, H. N. Gao, S. J. Zhu, T. Q. Wang, B. Yang, *Acs Appl. Mater. Inter.* **2012**, *4*, 2775.
[11] A. Mishra, P. Bauerle, *Angew. Chem.ntern. Ed.* **2012**, *51*, 2020.
[12] V. Gupta, A. K. K. Kyaw, D. H. Wang, S. Chand, G. C. Bazan, A. J. Heeger, *Sci Rep-Uk* **2013**, 3.
[13] T. S. van der Poll, J. A. Love, T. Q. Nguyen, G. C. Bazan, *Adv. Mater.* **2012**, *24*, 3646.
[14] A. K. K. Kyaw, D. H. Wang, V. Gupta, J. Zhang, S. Chand, G. C. Bazan, A. J. Heeger, *Adv. Mater.* **2013**, *25*, 2397.
[15] A. K. K. Kyaw, D. H. Wang, V. Gupta, W. L. Leong, L. Ke, G. C. Bazan, A. J. Heeger, *Acs Nano* **2013**, *7*, 4569.
[16] Y. Huang, W. Wen, S. Mukherjee, H. Ade, E. J. Kramer, G. C. Bazan, *Adv. Mater.* **2014**, *26*, 4168.
[17] T. A. M. Ferenczi, C. Muller, D. D. C. Bradley, P. Smith, J. Nelson, N. Stingelin, *Adv. Mater.* **2011**, *23*, 4093.
[18] A. K. K. Kyaw, D. H. Wang, C. Luo, Y. Cao, T. Q. Nguyen, G. C. Bazan, A. J. Heeger, *Adv. Energy Mater.* **2014**, 4.
[19] J. A. Love, C. M. Proctor, J. H. Liu, C. J. Takacs, A. Sharenko, T. S. van der Poll, A. J. Heeger, G. C. Bazan, T. Q. Nguyen, *Adv. Funct. Mater.* **2013**, *23*, 5019.
[20] W. Ma, J. Y. Kim, K. Lee, A. J. Heeger, *Macromol. Rapid Comm.* **2007**, *28*, 1776.
[21] E. Saracco, B. Bouthinon, J. M. Verilhac, C. Celle, N. Chevalier, D. Mariolle, O. Dhez, J. P. Simonato, *Adv. Mater.* **2013**, *25*, 6534.
[22] C. He, C. M. Zhong, H. B. Wu, R. Q. Yang, W. Yang, F. Huang, G. C. Bazan, Y. J. Cao, *Mater. Chem.* **2010**, *20*, 2617.
[23] F. Guo, X. D. Zhu, K. Forberich, J. Krantz, T. Stubhan, M. Salinas, M. Halik, S. Spallek, B. Butz, E. Spiecker, T. Ameri, N. Li, P. Kubis, D. M. Guldi, G. J. Matt, C. J. Brabec, *Adv. Energy Mater.* **2013**, *3*, 1062.